

Routine MRI With DWI Sequences to Detect Liver Metastases in Patients With Potentially Resectable Pancreatic Ductal Carcinoma and Normal Liver CT: A Prospective Multicenter Study

Anne-Marie Marion-Audibert¹
 Marie-Pierre Vullierme²
 Maxime Ronot²
 Jean-Yves Mabrut³
 Alain Sauvanet⁴
 Marc Zins⁵
 Muriel Cuilleron⁶
 Antonio Sa-Cunha^{7,8}
 Philippe Lévy⁹
 Agnès Rode¹⁰

OBJECTIVE. The purpose of this study was to evaluate the performance of systematic MRI with DWI for the detection of liver metastases (LM) in patients with potentially resectable pancreatic ductal carcinoma and normal liver findings at CT.

SUBJECTS AND METHODS. Patients with potentially resectable pancreatic ductal carcinoma and a normal liver at CT were enrolled in a prospective multicenter study between March 2011 and July 2013 and underwent preoperative MRI. The reference standard was pathologic analysis of detected hepatic lesions.

RESULTS. A total of 118 patients were enrolled. MRI depicted liver lesions that were not visible at CT in 16 patients. All lesions were visualized both with and without DWI. Lesions were LM in 12 (10.2%) patients and were confirmed in seven patients by preoperative biopsy, four by intraoperative frozen section, and one at 6-month follow-up evaluation after pancreatic resection. All but one liver metastatic lesion diagnosed with MRI were smaller than 10 mm. Four of 118 (3.4%) patients had a false-positive diagnosis of LM at MRI and remained LM free after a follow-up period of 24 months or longer. Three of 102 (2.9%) patients with normal MRI findings had subcapsular LM that were diagnosed intraoperatively. At follow-up, 99 of 118 (83.9%) patients were LM free after a mean of 24 months. The patient-based sensitivity of MRI for the detection of LM was 80.0% (95% CI, 51.9–95.7%); specificity, 96.1% (95% CI, 90.4–98.9%); positive predictive value, 75.0% (95% CI, 47.6–92.7%); and negative predictive value, 97.1% (95% CI, 91.6–99.4%).

CONCLUSION. Compared with CT, preoperative MRI improves the detection of LM in patients with potentially resectable pancreatic ductal carcinoma and may change management and the rate of unnecessary laparotomy and pancreatectomy for 10% of patients.

Keywords: DWI, liver metastases, MRI, pancreatic ductal carcinoma, surgery

doi.org/10.2214/AJR.18.19640

Received January 29, 2018; accepted after revision March 16, 2018.

A. Sa-Cunha is a member of the board of and has received payment for lectures and meeting expenses from Merck Serono; has received payment for lectures and meeting expenses from Roche; is a member of the board of Olympus; has received payment for meeting expenses from Eumedica and Novartis; and is a member of the board and has received payment for lectures from Celgene.

WEB

This is a web exclusive article.

AJR 2018; 211:W217–W225

0361–803X/18/2115–W217

© American Roentgen Ray Society

The detection of small liver metastases (LM) represents a major challenge during the staging of pancreatic ductal carcinoma. Thoracoabdominopelvic CT is the established imaging modality for staging [1, 2]. However, 13–23% of patients who undergo a surgical procedure are finally found to have disease that is unresectable because of arterial involvement, peritoneal carcinomatosis, or subcapsular LM that were not diagnosed

in the preoperative workup [1–8]. This poor predictive value was confirmed in a large meta-analysis [2] including 29 articles and 2171 patients that showed a summary positive predictive value of 81% for predicting resectability with CT. Thus, 19% of patients underwent unnecessary surgical exploration, mainly because of unidentified LM. FDG PET and staging laparoscopy have been proposed to improve patient selection, but their effectiveness has not been established. The

¹Department of Gastroenterology, Croix-Rousse University Hospital, Lyon, France.

²Department of Medical Imaging, Beaujon University Hospital, 100 Blvd Leclerc, Clichy-la-Garenne, 92110, France. Address correspondence to M. P. Vullierme (marie-pierre.vullierme@aphp.fr).

³Department of Digestive Surgery and Liver Transplantation, Croix-Rousse University Hospital, Lyon, France.

⁴Department of Digestive Surgery and Liver Transplantation, Beaujon University Hospital, Clichy-la-Garenne, France.

⁵Department of Medical Imaging, Saint-Joseph Hospital, Paris, France.

⁶Department of Medical Imaging, Nord University Hospital, Saint-Etienne, France.

⁷Department of Digestive Surgery and Liver Transplantation, University Hospital of Bordeaux, France.

⁸Present address: Department of Surgery, Institut Gustave Roussy, Villejuif, France.

⁹Department of Pancreatobiliary, Beaujon University Hospital, Clichy-la-Garenne, France.

¹⁰Department of Medical Imaging, Croix-Rousse University Hospital, Lyon, France.

relevance of FDG PET has not been confirmed because of the lack of sensitivity for the detection of LM smaller than 1 cm [3]. Although staging laparoscopy could be used to detect peritoneal metastases and small subcapsular LM, its use in routine practice has not been accepted because it is invasive, expensive, and time-consuming [4, 9].

The contrast resolution of MRI and the rate of detection of malignancies and focal lesions in the liver have been found to be better than those of CT, especially for the study of subcentimeter lesions in patients with potentially resectable pancreatic ductal carcinoma [5–8]. Of all available MRI sequences, DWI has been found to be highly sensitive for detecting focal liver lesions [6–15]. For instance, DWI depicts 20% more LM than does CT in patients with colorectal cancer or malignant melanoma [12, 16–19] and 15–25% more than T2-weighted or gadolinium chelate-enhanced MRI in patients with neuroendocrine tumors [17]. In a single-center retrospective study published in 2017, Kim et al. [18] found that systematic use of MRI in the preoperative workup of patients with pancreatic ductal carcinoma led to a significantly higher rate of detection of LM even in patients with normal liver results at CT. Those authors also reported better overall and progression-free survival rates and a lower recurrence rate in patients who underwent MRI. A more recent retrospective study [6] concluded that MRI with DWI has better diagnostic performance in characterization of indeterminate or suspicious metastases visualized at prospective CT of potentially resectable pancreatic ductal carcinoma, aiding in determination of appropriate surgical candidates. These results require validation in prospective multicenter studies.

The aim of our prospective study was to evaluate the added value of systematic routine preoperative MRI (comprising DWI) for the detection of LM in patients with potentially resectable pancreatic ductal carcinoma and normal liver findings at CT.

Subjects and Methods

Study Design

This national, prospective, multicenter, non-randomized study included the surgical oncology units of seven participating centers. Because suitable data reporting the rate of detection of LM in the setting of pancreatic ductal adenocarcinoma were not available when the study was initiated, we could not estimate the sample size. Yet, because LM were expected to be small (< 1 cm),

we relied on data published about small colorectal LM [15, 19]. These studies showed sensitivity of CT of approximately 50% and of DWI of approximately 70% for lesions smaller than 1 cm. With power of 80% and a 5% first-order error rate, the required sample size was estimated to be 91.

The local ethics committee of the Medical University of Lyon, France, approved the study, and it was registered at clinicaltrials.gov (NCT02896946). Informed consent was obtained from all participating patients.

Study Population

All consecutively registered patients with potentially resectable pancreatic ductal carcinoma were enrolled in the study between March 2011 and July 2013. The inclusion criteria were as follows: pancreatic mass histologically proven to be pancreatic ductal carcinoma before surgery (by biopsy) or by means of intraoperative biopsy or resection; contrast-enhanced thoracoabdominopelvic CT fulfilling the technical quality criteria of similar protocols across all centers (Tables 1 and 2) and performed with a maximal 1-month interval before surgery; presence of a pancreatic tumor considered to be either resectable (no encasement of celiac axis, superior mesenteric artery, or portal and mesenteric vein) or borderline according to the CT-based classification of the National Comprehensive Cancer Networks (version 2.2010 updated to 2.2012) [4] and previously treated with chemotherapy with or without radiotherapy with no extrapancreatic metastases; confirmation of resectable pancreatic ductal carcinoma at a multidisciplinary team meeting. If neoadjuvant therapy was provided, the patient was included in the study on the basis of assessment during a second multidisciplinary team meeting after neoadjuvant treatment was complete.

TABLE 1: MDCT Parameters

Parameter	Sensation 16 (8 + 2) ^a	LightSpeed VCT (48 + 24 + 4) ^a	Brilliance (26 + 4) ^a
No. of channels	16	64	40
Section collimation ^b	16 × 0.75	64 × 0.625	40 × 0.625
Section thickness (mm)	0.9–1.25	1.25	1.25
Noise index	19–21	19–21	19–21
Reconstruction interval (mm)	0	0	0
Pitch	1	1	1
Tube current (mAs)	Reference current (mA)	Automatic modulation	Reference image
Rotation time (s)	0.5	0.6	0.75
Tube voltage (kVp)	120	120	120
Matrix	512 × 512	512 × 512	512 × 512

Note—Sensation (Siemens Healthcare), LightSpeed VCT (GE Healthcare), Brilliance (Philips Healthcare).

^aValues in parentheses are numbers of patients who underwent imaging with the scanner model at individual institutions.

^bNumber of detector rows multiplied by detector collimation in millimeters.

The exclusion criteria were age younger than 18 years, general contraindication to pancreatic surgery, LM detected at CT, and CT findings of locally advanced cancer.

The following parameters were also recorded for each patient at each of the seven centers: age, sex, carbohydrate antigen 19-9 (CA 19-9) serum level, serum conjugated bilirubin level, presence of jaundice, preoperative biliary drainage, use and type of neoadjuvant therapy, and second centralized reading.

Thoracoabdominopelvic CT Protocol

All patients underwent a thoracoabdominopelvic CT examination that fulfilled the quality criteria in Table 1. Brilliance 40 CT (Philips Healthcare), Somatom Sensation 16 (Siemens Healthcare), and LightSpeed VCT 64 (GE Healthcare) scanners were used. Standard procedures for operating a multislice triphase MDCT scanner were used at all participating centers. Dose modulation software was used to determine the tube current–time product (milliampere-seconds) of each vendor (noise index, 19–21, 100–660 mA) [20]. After an initial unenhanced CT acquisition, 2 mL/kg of a low-osmolar contrast agent (350–400 mg I/mL) was injected at a flow rate of 3–4 mL/s. After 45 seconds (during the late arterial, or so-called pancreatic, phase), reconstruction was performed with a slice thickness of 1.25 mm or less, fully covering the liver and pancreas, including retroreconstruction with a narrow FOV focused on the pancreas. After 70–80 seconds, venous phase thoracoabdominopelvic CT was performed. All images were archived in permanent storage. The following parameters of the pancreatic tumor were recorded at preoperative CT: size in millimeters, site of pancreatic ductal carcinoma, and vascular encasement of each vessel.

MRI of Liver Metastases of Pancreatic Ductal Carcinoma

MRI Protocol

All MRI examinations were performed with a Magnetom Avanto Syngo MR B15 1.5 T (Siemens Healthcare), an Intera 1.5 T (Philips Healthcare), or a Signa 1.5-T (GE Healthcare) system. MRI was performed less than 21 days before surgery. Standard operating procedures were applied at all participating research centers for coverage of the liver and the pancreas (Table 2). The extracellular gad-

olinium chelate gadoteric acid (Dotarem, Guerbet) was used and delivered through an automatic injector at a dose of 0.1 mL/kg and a rate of 3 mL/s followed by a 20 mL flush of saline solution.

The DWI sequences covering the liver and pancreas were performed with respiratory gating. Apparent diffusion coefficient (ADC) maps were generated at low (0 or 50 s/mm²), intermediate (150 or 400 s/mm²), and high (600 or 800

s/mm²) b values. ADC maps were automatically calculated by monoexponential fit with different available b values.

Interpretation of Imaging Data

Images were dispatched to a PACS (Carestream, Kodak PACS) for blinding to clinical data, imaging follow-up, and histologic result review. Two sets of populations were reviewed, most not being

TABLE 2: MRI Parameters

Parameter	Sequence			
	T1-Weighted	T2-Weighted	DWI	Dynamic Imaging
Intera 1.5 T		HASTE		Thrive
TR/TE (ms)	6.6/2.1	1500/108	2200/79	4/2.1
Echo-train length	1	1	1	1
Flip angle (°)	75	90	90/180	10
Slice thickness/spacing (mm)	5/0	4/1	5/1	5.4/0
FOV (mm)	350 × 350–360 × 360	350 × 263	380 × 380	360 × 360
Asset factor				
No. of signals averaged	1	1	2	1
Fat saturation				
Matrix size	320 × 224	256 × 192	192 × 115	256 × 211
b Value (s/mm ²)			0, 150, 600, or 800	
Signa 1.5 T		Fat saturated		LAVA
TR/TE (ms)	210/1.7	2100/89.2	3000/63.5	2.28/1.05
Echo-train length	1	16	1	1
Flip angle (°)	80		90/180	80
Slice thickness/spacing (mm)	2.4	4/1	5/1	2.4
FOV (mm)	340 × 340	340 × 340	400 × 400	350 × 350
Asset factor	2	2	2	2
No. of signals averaged	1	2	8	1
Fat saturation		Yes		
Matrix size	288 × 192	256 × 224	160 × 160	288 × 192
b Value (s/mm ²)			0 or 50, 150 or 400, 600 or 800	
Magnetom Aera 1.5 T	GRAPPA 2	Fat saturated		VIBE (GRAPPA 2)
TR/TE (ms)	162/6.16	2100/81	2500/79	3.81/1.31
Echo-train length	2	1	58	2
Flip angle (°)	70		90/180	12
Slice thickness/spacing (mm)	4	6/1	5/0.5	3
FOV (mm)	300 × 300	350 × 350	350 × 262	420 × 312
Asset factor	2	2	2	2
No. of signals averaged	1	1	8	1
Fat saturation	Water selection	Yes, high	SPAIR	Yes, quick
Matrix size	288 × 192	384 × 207	128 × 128	384 × 192
b value (s/mm ²)			50, 400, 600, and 800	

Note—Intera 1.5 T (Philips Healthcare), Signa 1.5 T (GE Healthcare), 1.5-T, Magnetom Aera MR B15 1.5 T (Siemens Healthcare). LAVA = liver acquisition with volume acceleration, GRAPPA = generalized auto calibrating partially parallel acquisition, VIBE = volumetric interpolated breath-hold examination, SPAIR = spectral attenuated inversion recovery.

centralized. Three radiologists (one from each of the three largest recruiting centers) specialized in abdominal imaging (each with more than 10 years of experience) reviewed the data on 24, 48, and 26 patients at their own high-volume centers. The second set, collected at the other four recruiting centers, was a small-volume population and included four, two, eight, and four patients, whose images were centrally analyzed by two readers. Readings were performed independently on a per-center basis. CT was interpreted separately from MRI with a minimum 2-week delay between CT and MRI readings. The four readers completed data reports for both CT and MRI. For each patient, readers were asked to state whether LM were present or absent. Lower b values were used for lesion detection, and their presence was confirmed on high b value images [21].

A typical liver metastasis was defined as the presence of a focal lesion visible on an MR image with any of the following features: mild or moderate signal hyperintensity on T2-weighted images, mild or moderate hypointensity on T1-weighted images, or poor contrast uptake after injection of gadolinium chelate, that is, possible peripheral rim enhancement. The typical aspect on DW images was combined increasing hyperintensity from b0 to b600–b800 and ADC values that were visually lower than those of surrounding liver. Lesions with any other features were considered questionable LM, especially if ADC values were not low or could not be clearly determined because of the small size of the lesion. The following parameters were recorded for each lesion detected at MRI: number, location with a detailed map of each lesion, size, and ADC qualitative values compared with surrounding liver parenchyma.

Final Diagnosis

The reference standard for a positive diagnosis of LM was pathologic analysis. If a suspected liver metastasis was detected, percutaneous ultrasound-guided biopsy was attempted. Only one lesion was biopsied if multiple lesions were present. If the target lesion was found to be malignant, surgery was cancelled. If percutaneous biopsy was not technically feasible, surgical exploration was undertaken.

Each center applied a standardized surgical protocol defined by experts in pancreatic surgery. The procedure included initial exploration of the peritoneum and the liver by bilobar manual palpation followed by intraoperative ultrasound. Special attention was paid to atypical hepatic lesions identified at preoperative MRI. Any intraoperatively identified lesion was biopsied and sent for immediate frozen-section examination to search for evidence of malignancy. If the target lesion was found to be

malignant, pancreatic resection was contraindicated. If no tissue samples were available, patients underwent clinical and CT follow-up every 3 months for 2 years, and the final diagnosis was based on these 2-year follow-up findings.

Data Expression and Statistical Analysis

All clinical and imaging data were centralized. Categorical variables were expressed as counts and percentages and continuous variables as median values with ranges. The performance of MRI with DWI was assessed on the basis of the following indexes: sensitivity, specificity, positive predictive value, negative predictive value, and accuracy, expressed in percentages with 95% CIs. The calculations were based on binomial distribution and were made on a per-patient basis. All

tests were two-sided, and $p < 0.05$ was considered significant. Analysis was performed with SAS software (version 9.2, SAS Institute).

Results

Patient Baseline Characteristics

A total of 118 patients were enrolled during the study period. Their baseline characteristics are shown in Table 3. Sixteen (16/118 [13.6%]) patients had a borderline tumor and underwent neoadjuvant therapy (chemoradiation therapy, 12; chemotherapy alone, four). These patients were reassessed after neoadjuvant treatment was completed and were considered to have resectable pancreatic ductal carcinoma after CT showed that the disease was controlled.

TABLE 3: Baseline Patient Characteristics

Variable	Data
Age (y)	64.4 (36–87)
Sex (no.)	
Men	64 (45.8)
Women	54 (54.2)
Size of pancreatic primary tumor on MR images (mm)	23 (10–38)
Tumor location	
Head or neck	78 (66.1)
Body or tail	33 (28.0)
Uncinate process	7 (5.9)
Clinical jaundice	53 (44.9)
Background of chronic pancreatitis	11 (9.3)
CA 19-9 level (U/L)	1794 (2–3442)
Conjugated bilirubin (mmol/L)	181.5 (1–557)
Preoperative endoscopic biliary drainage	
Total procedures	38 (32.2)
Metallic stent	23 (19.5)
Plastic stent	15 (12.7)
Neoadjuvant therapy	
All types	16 (13.6)
Chemotherapy + radiation therapy	12 (10.2)
Chemotherapy alone	4 (3.4)
Chemotherapy regimen	
Gemcitabine + oxaliplatin	9 (7.6)
Gemcitabine	7 (5.9)
Radiation dose delivered (Gy)	50 (45–54)
Surgical procedure	
Not performed	7 (5.9)
Open-close surgical exploration	18 (15.3)
Pancreatic excision with curative intent	93 (78.8)

Note—Values are count and percentage or median value and range. CA 19-9 = carbohydrate antigen 19-9.

Identification of Focal Liver Lesions With MRI

MRI showed that 16 of 118 (13.6%) patients had either typical (11/118 [9.3%]) or questionable (5/118 [4.2%]) hepatic lesions for the diagnosis of LM. Seven of the 11 patients with typical hepatic lesions underwent preoperative ultrasound-guided percutaneous biopsy, which showed histologic evidence of malignancy. Those patients did not undergo surgery. The other four patients with typical LM and all five patients with questionable hepatic lesions did not undergo preoperative biopsy because lesions were not visible at ultrasound. They therefore underwent surgical exploration.

Thus, a total of 111 of 118 (94.1%) patients underwent surgical exploration (Fig. 1), including 102 (86.4%) patients with no suspected LM at preoperative MRI. Eleven of these 111 patients (9.3% of the total 118) were found to have locally advanced disease contraindicating resection. Therefore, only surgical exploration or palliative bypass was performed. None of the patients who underwent surgical exploration or palliative bypass had lesions detected at preoperative MRI.

Intraoperative targeted biopsy was successfully performed on the four patients with typical LM at preoperative MRI that could not be sampled with percutaneous biopsy (Fig. 2). The diagnosis of LM was confirmed intraoperatively, and pancreatic resection was cancelled for all of them.

None of the five patients with questionable hepatic lesions at preoperative MRI underwent intraoperative biopsy, because lesions were not visible with intraoperative ultrasound. All of these patients underwent pancreatic resection. During follow-up 6 months after surgery, one of the five presented with a liver metastatic lesion at the same location as the initial questionable lesion. The 12 patients with true-positive results had typical or questionable DWI patterns; 11 had a typical pattern. The other four (3.4% of the 118) patients with questionable hepatic lesions at preoperative MRI had false-positive findings at MRI both with and without DWI and remained LM free at 24 months (Fig. 3). Their DWI patterns did not fulfill all features required. In particular, ADC values were not visually lower than those of surrounding liver.

Three of 102 (2.9%) patients had false-negative MRI findings. They were found to have a single subcapsular lesion (5 or 6 mm) during surgery that was confirmed to be malignant at frozen section analysis.

A total of 93 of the 118 (78.8%) patients with no intraoperative evidence of locally ad-

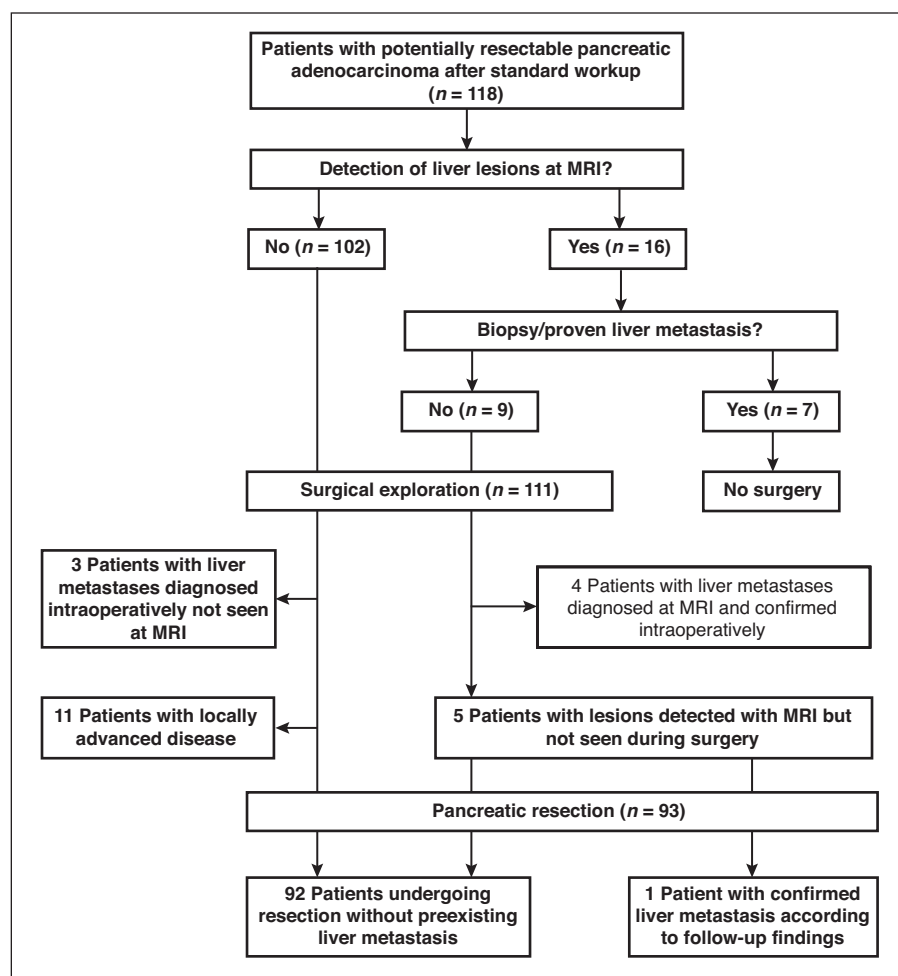


Fig. 1—Study flowchart shows enrollment of patients with contrast-enhanced CT showing potentially resectable pancreatic ductal carcinoma, fulfilling technical quality criteria according to protocols similar across all centers and normal liver CT findings.

vanced or metastatic disease underwent pancreatic resection. The histologic characteristics are shown in Table 4. Liver lesions detected at MRI were not seen at retrospective review of the CT images. At follow-up, 99 of 118 (83.9%) patients were LM free after a mean of 24 months.

Aspects of Liver Metastases on MRI

A total of 17 LM were correctly identified with MRI in 12 (10.2%) patients, including 11 (9.3%) patients with typical LM lesions and one with a questionable lesion. Solitary lesions were found in five patients and multiple lesions in seven. The median tumor size was 5.2 mm (range, 4–11 mm). Six tumors measured 4 mm; two, 5 mm; eight, 6–9 mm; and only one tumor (11 × 9 mm) was larger than 10 mm. All LM were hyperintense on high-b-value DW images (Fig. 2), and ADC values were lower than those of surrounding liver parenchyma in all but one case.

Patient-level analysis showed that 16 patients had lesions visualized with both DWI and other sequences. In 12 of them, lesions had marked hypointensity on the ADC map. In the other four, the lesions did not exhibit such hypointensity on the ADC maps. Three of these four lesions were false-positive. Therefore, only one patient had a true-positive liver metastatic lesion that was visible with both DWI and other MRI sequences but on the ADC maps was not markedly hypointense compared with surrounding liver.

Lesion-level analysis showed that 17 metastases were visualized in total and that none were seen with other sequences but not DWI. Three lesions were missed with all sequences.

Diagnostic Performance of MRI With DWI

Twelve of the 16 hepatic lesions detected with MRI were found to be true-positive findings, and four were false-positive

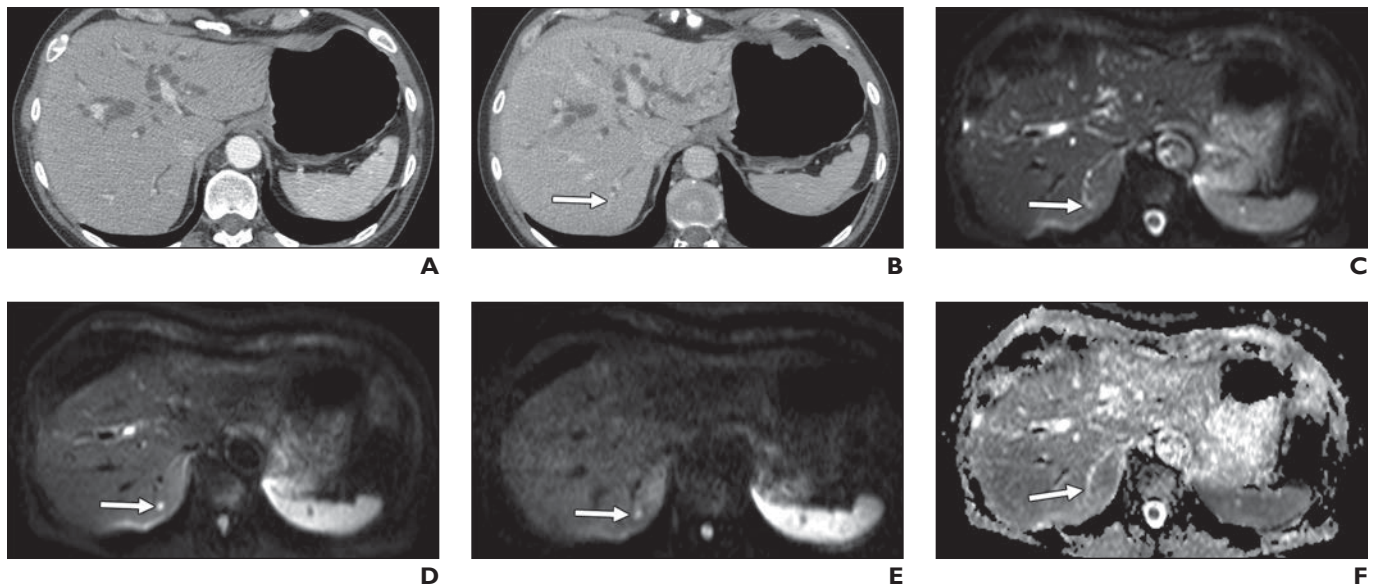


Fig. 2—56-year-old man with potentially resectable pancreatic adenocarcinoma undergoing preoperative imaging consisting of CT followed by MRI. Lesion was biopsied during surgery.

- A**, Arterial pancreatic phase CT image does not show lesion.
B, Venous phase CT image does not show lesion (*arrow*), which is obscured by enlarged bile ducts.
C, DW image at b0 shows 7-mm metastatic lesion (*arrow*) in liver segment VII.
D, DW image at b150 shows 7-mm metastatic lesion (*arrow*) in segment VII has higher signal intensity than it does in **C**.
E, DW image at b600 shows 7-mm metastatic lesion (*arrow*) has higher signal intensity than it does in **C** and **D**.
F, DW image shows 7-mm lesion (*arrow*) has apparent diffusion coefficient value lower than that of surrounding liver.

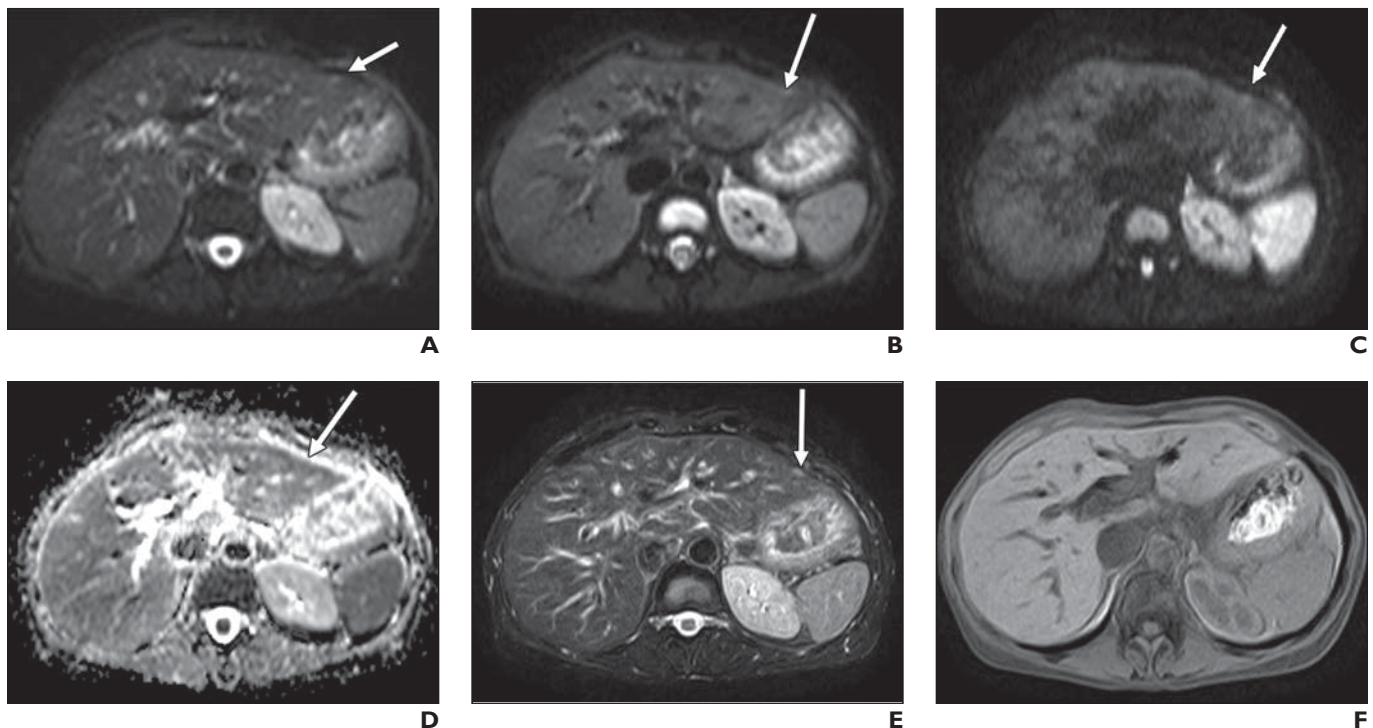


Fig. 3—45-year-old woman with potentially resectable pancreatic adenocarcinoma undergoing preoperative imaging. Example of hepatic lesion undetectable at CT and false-positive MRI finding. Lesion was not seen at surgery. Five years after surgery patient was alive without left lobe liver metastasis or peritoneal nodule in this location.

- A**, DW image at b0 shows doubtful hyperintense subcapsular lesion (*arrow*) in segment III.
B, DW image at b150 shows doubtful hyperintense subcapsular lesion (*arrow*) in segment III.
C, DW image at b600 shows doubtful hyperintense subcapsular lesion (*arrow*) in segment III.
D, Apparent diffusion coefficient map shows 5-mm isointense pseudolesion (*arrow*).
E, T2-weighted MR image shows moderately hyperintense pseudolesion (*arrow*).
F, T1-weighted MR image does not show lesion.

Downloaded from www.ajronline.org by UBC Library Central Serials on 05/03/19 from IP address 142.103.160.110. Copyright ARRS. For personal use only; all rights reserved

MRI of Liver Metastases of Pancreatic Ductal Carcinoma

TABLE 4: Histologic Characteristics of the Primary Pancreatic Tumor

Variable	Result
Histologic type	
Ductal carcinoma	107 (90.7)
Malignant invasive intraductal papillary mucinous neoplasm	11 (9.3)
Pathologic TNM classification	
No specimen	25 (21.2)
Specimen available	93 (78.8)
pT1N0	4 (4.3)
pT2N0	4 (4.3)
pT2N1	3 (3.2)
pT3N0	29 (31.2)
pT3N1	49 (52.7)
pT4N0	3 (3.3)
pT4N1	1 (1.0)
Radicality of resection	
No resection	25 (21.2)
R0	89 (75.4)
R1	4 (3.4)

Note—Values are count with percentage in parentheses.

(Table 5). Those four patients had one lesion each, measuring 3 to 11 mm. All four lesions were hyperintense on high-b-value DW images, but the ADC values were not lower than those of surrounding liver parenchyma. These lesions were also visible with other MRI sequences. Table 5 shows the diagnostic value of MRI for the detection of LM in a per-patient analysis. The sensitivity of MRI for typical LM lesions was 73.3% and the specificity, 100%. The sensitivity and specificity when questionable lesions were included were 80.0% and 96.1%. The negative predictive value was 96.2% when only typical lesions were included and 97.1% when both typical and atypical lesions were included.

Discussion

To our knowledge this study is the largest prospective multicenter assessment of the contribution of routine MRI with DWI sequences to the detection of LM in patients with potentially resectable pancreatic ductal carcinoma and normal liver findings at abdominal CT. MRI, especially DWI, has been found to depict small LM that are undetectable with standard workup CT in approximately 10% of patients, leading to a change in management [5, 6, 12]. This was well documented in a recent retrospective study of potentially resectable pancreatic ductal carcinoma that was LM negative at CT but at MRI was found to have LM in 2–3% of cases [6].

In the current study, MRI depicted 17 LM in 12 of 118 patients with sensitivity of 80.0% for both typical and questionable lesions detected with DWI and sensitivity of 73.3% for typical lesions only. When ADC was lower than that of surrounding liver (typical lesion), specificity was 100%. This visually low ADC helped us to be confident of our LM diagnoses. The suspected lesions in 12 patients were all confirmed to be LM at histologic analysis. After retrospective review of available imaging results, lesions were still invisible on CT images, and only 11 were identified on MR images without ADC being low at DWI. Surgery was prevented in seven patients, and unnecessary pancreatic resection was avoided in four other patients in whom targeted biopsy based on findings of MRI with DWI yielded a diagnosis of LM during exploratory laparotomy. Thus, unnecessary pancreatectomy was avoided in 11 of 118 patients.

Detection of LM is a major challenge in the selection of patients with pancreatic ductal carcinoma, and there is no clearly validated staging modality. In a retrospective study including 76 patients with suspected pancreatic ductal carcinoma, Valls et al. [8] found that the main (55.5%) reason for not resecting lesions initially believed to be resectable according to the CT findings was unsuspected LM identified during surgery. Interestingly, the average size of unidentified LM was 8 mm. LM secondary to pancreatic ductal carcinoma are reportedly small, mostly hypovascular, and located in the subcapsular area of the liver in 80% of patients, possibly owing to locoregional peritoneal dissemination [5, 10]. These features may play a role in the poor performance of CT and FDG PET/CT. The sensitivity of FDG PET/CT in lesions smaller than 1 cm is no more than 21% [3]. On the other hand, exploratory laparoscopy

TABLE 5: Diagnostic Performance of MRI With DWI Among Patients With Potentially Resectable Pancreatic Ductal Carcinoma at Standard Workup in a Series of 15 Patients With Liver Metastases and 103 Without Metastases

Performance Measure	Diagnosis of Liver Metastasis Considered Only for Typical Lesions ^a	Diagnosis of Liver Metastasis Considered for Both Typical and Atypical Lesions ^b
Sensitivity	73.3 (44.9–92.2)	80.0 (51.9–95.7)
Specificity	100.0 (96.5–100.0)	96.1 (90.4–98.9)
Positive predictive value	100.0 (71.5–100.0)	75.0 (47.6–92.7)
Negative predictive value	96.2 (90.7–99.0)	97.1 (91.6–99.4)
Accuracy	96.6 (91.6–99.1)	94.1 (88.2–97.6)

Note—Values are percentages with 95% CI in parentheses. Typical lesions were defined as hyperintense lesions visualized on high-b-value DW images with apparent diffusion coefficient restriction. Atypical lesions were defined as hyperintense nodular lesion with uncertain diffusion restriction.

^aTrue-positive, 11; false-positive, 0; false-negative, 4; true-negative, 100.

^bTrue-positive 12, false-positive 4, false-negative, 3; true-negative, 99.

may be helpful before laparotomy is considered [9]. In the current study, however, as many as 75% of LM detected with MRI were in deep locations, limiting interest in primary laparoscopic exploration.

Over the past 5 years, the role of MRI with DWI sequences for the detection of small LM has been suggested for other primary tumors, such as colorectal cancers and pancreatic neuroendocrine tumors [17]. This technique can be used to differentiate underlying liver parenchyma and malignant lesions on the basis of decreased diffusion of water molecules caused by tumoral hypercellularity and reduced extracellular space. Because of the black-blood effect on vessels and low risk of motion artifacts, DWI is especially useful for the detection of small (< 10 mm) metastatic lesions and is more sensitive and more accurate than conventional imaging with T2-weighted techniques [11, 22]. Furthermore, analysis of the liver is improved on high-b-value images because of the decrease in signal intensity of dilated biliary ducts. In a retrospective study, Parikh et al. [15] found that the DWI sequence was better than standard breath-hold T2-weighted MRI for the detection of colorectal LM (88% vs 70%, $p < 0.05$). Similar findings were suggested in a meta-analysis by Wu et al. [23]. Other studies comparing the performance of CT and DWI for the staging of pancreatic ductal carcinoma and colorectal cancer showed that DWI increased the rate of LM detection and was more accurate for characterization of benign lesions, such as cysts and hemangiomas, especially those smaller than 10 mm [6, 24]. Although CT is not accurate for classification of small lesions with low attenuation of 30–60 HU, DWI can be used to differentiate metastatic lesions from cysts or hemangiomas because of differences in cellularity and ADC values [6, 24–26].

Kim et al. [12] and Holzapfel et al. [27] performed two studies comparing the results of CT and DWI for the detection of LM in pancreatic cancers. The first study, completed by Holzapfel et al. in 2011, was a single-center prospective study with a cohort of 31 patients who had neuroendocrine tumors, acinar cell carcinomas, and intraductal papillary mucinous neoplasms. None of the included patients had normal liver findings at CT. In that study, DWI depicted LM that had been undiagnosed at CT in 4 of 31 patients (12.9%), resulting in a change in therapeutic strategy. Kim et al. conducted a retrospective study and found that the use of liver

DWI during the preoperative evaluation resulted in detection of LM in three of 58 patients (5%) without hepatic lesions at CT and in 17 of 53 patients (32%) with undefined hepatic lesions at CT.

Adding MRI to the evaluation of all patients could be questionable as a cost-effective strategy. However, laparoscopy is invasive, expensive, and time-consuming [9]. Pancreatectomy has a 20–35% morbidity rate and 3–15% mortality rate and is not associated with a higher survival rate if LM are present [2, 28]

Our study had limitations. First, MRI was not performed with a liver-specific contrast agent, such as gadoxetic acid. Gadoxetic acid improves contrast resolution in the liver owing to an increased signal gradient between normal liver, which is enhancing, and LM, which are not. Sensitivity for the detection of LM from colorectal and pancreatic cancers has been found to be excellent with DWI and gadoxetic acid administration, and use of this technique and agent probably resulted in a higher detection rate [29, 30–32]. Moreover, we did not compare results of MRI with or without DWI, nor did we analyze DWI alone because the added value of DWI for the detection of focal liver lesions has been found numerous times. We aimed at assessing the value of MRI including DWI as an entire workup examination in the context of pancreatic ductal adenocarcinoma before resection. We also did not compare the results of DWI with those of PET/CT, which is relevant for the detection of distant metastases. However, the sensitivity of PET/CT is only 45–70% for the detection of LM and even lower for metastases smaller than 10 mm [3, 33]. Moreover, this study included a large number of patients and was prospective, preventing potential biases related to retrospective review of imaging findings.

Conclusion

The current study showed that routine use of MRI with DWI resulted in the detection of small LM. It also resulted in a change in therapeutic strategy for 10% of patients with potentially resectable pancreatic ductal carcinoma and normal liver findings at CT. Thus, MRI with DWI should be systematically included in preoperative staging for these patients.

References

1. Maire F, Sauvanet A, Trivin F, et al. Staging of pancreatic head adenocarcinoma with spiral CT and endoscopic ultrasonography: an indirect eval-

uation of the usefulness of laparoscopy. *Pancreatology* 2004; 4:436–440

2. Somers I, Bipat S. Contrast-enhanced CT in determining resectability in patients with pancreatic carcinoma: a meta-analysis of the positive predictive values of CT. *Eur Radiol* 2017; 27:3408–3435
3. Heinrich S, Goerres GW, Schäfer M, et al. Positron emission tomography/computed tomography influences on the management of resectable pancreatic cancer and its cost-effectiveness. *Ann Surg* 2005; 242:235–243
4. Tempero MA, Arnoletti JP, Behrman SW, et al. Pancreatic adenocarcinoma, version 2.2012: featured updates to the NCCN Guidelines. *J Natl Compr Canc Netw* 2012; 10:703–713
5. Elnahal SM, Shinagare AB, Szymonifka J, Hong TS, Enzinger PC, Mamon HJ. Prevalence and significance of subcentimeter hepatic lesions in patients with localized pancreatic adenocarcinoma. *Pract Radiat Oncol* 2012; 2:e89–e94
6. Jeon SK, Lee JM, Joo I, et al. Magnetic resonance with diffusion-weighted imaging improves assessment of focal liver lesions in patients with potentially resectable pancreatic cancer on CT. *Eur Radiol* 2018; 28:3484–3493 [Erratum in *Eur Radiol* 19 April 2018]
7. Tempero MA, Malafa MP, Al-Hawary M, et al. Pancreatic adenocarcinoma, version 2.2017, NCCN Clinical Practice Guideline in Oncology. *J Natl Compr Canc Netw* 2017; 15:1028–1061
8. Valls C, Andía E, Sanchez A, et al. Dual-phase helical CT of pancreatic adenocarcinoma: assessment of resectability before surgery. *AJR* 2002; 178:821–826
9. Pisters PW, Lee JE, Vauthey JN, Charnsangavej C, Evans DB. Laparoscopy in the staging of pancreatic cancer. *Br J Surg* 2001; 88:325–337
10. Danet IM, Semelka RC, Nagase LL, Woosely JT, Leonardou P, Armao D. Liver metastases from pancreatic adenocarcinoma: MR imaging characteristics. *J Magn Reson Imaging* 2003; 18:181–188
11. Bruegel M, Gaa J, Waldt S, et al. Diagnosis of hepatic metastasis: comparison of respiration-triggered diffusion-weighted echo-planar MRI and five T2-weighted turbo spin-echo sequences. *AJR* 2008; 191:1421–1429
12. Kim HJ, Lee SS, Byun JH, et al. Incremental value of liver MR imaging in patients with potentially curable colorectal hepatic metastasis detected at CT: a prospective comparison of diffusion-weighted imaging, gadoxetic acid-enhanced MR imaging, and a combination of both MR techniques. *Radiology* 2015; 274:712–722
13. Manenti G, Di Roma M, Mancino S, et al. Malignant renal neoplasms: correlation between ADC values and cellularity in diffusion weighted magnetic resonance imaging at 3 T. *Radiol Med (Torino)* 2008; 113:199–213
14. Matoba M, Tonami H, Kondou T, et al. Lung car-

MRI of Liver Metastases of Pancreatic Ductal Carcinoma

- cinoma: diffusion-weighted MR imaging—preliminary evaluation with apparent diffusion coefficient. *Radiology* 2007; 243:570–577
15. Parikh T, Drew SJ, Lee VS, et al. Focal liver lesion detection and characterization with diffusion-weighted MR imaging: comparison with standard breath-hold T2-weighted imaging. *Radiology* 2008; 246:812–822
16. Laurent V, Trausch G, Bruot O, Olivier P, Felblinger J, Regent D. Comparative study of two whole-body imaging techniques in the case of melanoma metastases: advantages of multi-contrast MRI examination including a diffusion-weighted sequence in comparison with PET-CT. *Eur J Radiol* 2010; 75:376–383
17. d'Assignies G, Fina P, Bruno O, et al. High sensitivity of diffusion-weighted MR imaging for the detection of liver metastases from neuroendocrine tumors: comparison with T2-weighted and dynamic gadolinium-enhanced MR imaging. *Radiology* 2013; 268:390–399
18. Kim HW, Lee JC, Paik KH, et al. Adjunctive role of preoperative liver magnetic resonance imaging for potentially resectable pancreatic cancer. *Surgery* 2017; 161:1579–1587
19. Nickel MC, Bipat S, Stoker J. Diagnostic imaging of colorectal liver metastases with CT, MR imaging, FDG PET, and/or FDG PET/CT: a meta-analysis of prospective studies including patients who have not previously undergone treatment. *Radiology* 2010; 257:674–684
20. Lee CH, Goo JM, Lee HJ, et al. Radiation dose modulation techniques in the multidetector CT era: from basics to practice. *RadioGraphics* 2008; 28:1451–1459
21. Coenegrachts K, Delanote J, Ter Beek L, et al. Improved focal liver lesion detection: comparison of single-shot diffusion-weighted echoplanar and single-shot T2 weighted turbo spin echo techniques. *Br J Radiol* 2007; 80:524–531
22. Zech CJ, Herrmann KA, Dietrich O, Horger W, Reiser MF, Schoenberg SO. Black-blood diffusion-weighted EPI acquisition of the liver with parallel imaging: comparison with a standard T2-weighted sequence for detection of focal liver lesions. *Invest Radiol* 2008; 43:261–266
23. Wu LM, Hu J, Gu HY, Hua J, Xu JR. Can diffusion-weighted magnetic resonance imaging (DW-MRI) alone be used as a reliable sequence for the preoperative detection and characterisation of hepatic metastases? A meta-analysis. *Eur J Cancer* 2013; 49:572–584
24. Eiber M, Fingerle AA, Brügel M, Gaa J, Rummeny EJ, Holzapfel K. Detection and classification of focal liver lesions in patients with colorectal cancer: retrospective comparison of diffusion-weighted MR imaging and multi-slice CT. *Eur J Radiol* 2012; 81:683–691
25. Bruegel M, Rummeny EJ. Hepatic metastases: use of diffusion-weighted echo-planar imaging. *Abdom Imaging* 2010; 35:454–461
26. Holzapfel K, Bruegel M, Eiber M, et al. Characterization of small (≤ 10 mm) focal liver lesions: value of respiratory-triggered echo-planar diffusion-weighted MR imaging. *Eur J Radiol* 2010; 76:89–95
27. Holzapfel K, Reiser-Erkan C, Fingerle AA, et al. Comparison of diffusion-weighted MR imaging and multidetector-row CT in the detection of liver metastases in patients operated for pancreatic cancer. *Abdom Imaging* 2011; 36:179–184
28. Wente MN, Veit JA, Bassi C, et al. Postpancreatectomy hemorrhage (PPH): an International Study Group of Pancreatic Surgery (ISGPS) definition. *Surgery* 2007; 142:20–25
29. Ito T, Sugiura T, Okamura Y, et al. The diagnostic advantage of EOB-MR imaging over CT in the detection of liver metastasis in patients with potentially resectable pancreatic cancer. *Pancreatology* 2017; 17:451–456
30. Motosugi U, Ichikawa T, Morisaka H, et al. Detection of pancreatic carcinoma and liver metastases with gadoxetic acid-enhanced MR imaging: comparison with contrast-enhanced multi-detector row CT. *Radiology* 2011; 260:446–453
31. Chung WS, Kim MJ, Chung YE, et al. Comparison of gadoxetic acid-enhanced dynamic imaging and diffusion-weighted imaging for the preoperative evaluation of colorectal liver metastases. *J Magn Reson Imaging* 2011; 34:345–353
32. Vilgrain V, Esvan M, Ronot M, Caumont-Prim A, Aubé C, Chatellier G. A meta-analysis of diffusion-weighted and gadoxetic acid-enhanced MR imaging for the detection of liver metastases. *Eur Radiol* 2016; 26:4595–4615
33. Higashi T, Saga T, Nakamoto Y, et al. Diagnosis of pancreatic cancer using fluorine-18 fluorodeoxyglucose positron emission tomography (FDG PET): usefulness and limitations in “clinical reality.” *Ann Nucl Med* 2003; 17:261–279